

A Cyano-Substituted Organoboron Electron-deficient Building Block for D-A Type Conjugated Polymers

Meng-Yu Liu^{a,b,†}, Xing-Xin Shao^{a,b,†}, Jun Liu^{a,b,*}, and Li-Xiang Wang^{a,b}

^a State Key Laboratory of Polymer Physics and Chemistry, Changchun Institute of Applied Chemistry, Chinese Academy of Sciences, Changchun 130022, China

^b School of Applied Chemistry and Engineering, University of Science and Technology of China, Hefei 230026, China

 Electronic Supplementary Information

Abstract The development of donor-acceptor (D-A) type conjugated polymers depends largely on the design of novel A building blocks. Herein, we report a novel A building block based on the cyano-substituted organoboron unit (**SBN-3**). Compared with the most common fluorine-substituted B←N unit, **SBN-3** displays a significantly downshifted LUMO energy level because of the strong electron-withdrawing ability of cyano groups. In addition, due to the greater impact of cyano substitution on LUMO than on HOMO, **SBN-3** exhibits a reduced band gap, near-infrared absorption and fluorescence properties. The D-A type conjugated polymers based on the cyano-substituted B←N unit with thiophene-based units show narrow optical band gaps of ca. 1.3 eV as well as distinctive electronic structures, *i.e.*, delocalized LUMOs and localized HOMOs. This work thus provides not only an effective approach to design strong A units but also a new electron-deficient building block for D-A type conjugated polymers.

Keywords Cyano-substituted; B←N unit; Building block; Narrow band gap; D-A type conjugated polymers

Citation: Liu, M. Y.; Shao, X. X.; Liu, J.; Wang, L. X. A cyano-substituted organoboron electron-deficient building block for D-A type conjugated polymers. *Chinese J. Polym. Sci.* 2023, 41, 832–838.

INTRODUCTION

Conjugated polymers with delocalized π -electrons have attracted considerable attention in the last few decades, because of their distinctive optical, electronic and magnetic properties in the neutral or doped state.^[1–4] In particular, D-A type conjugated polymers play an important role in high-performance organic optoelectronic devices, such as organic field-effect transistors (OFETs), organic solar cells (OSCs), and organic photodetectors, due to their great advantages of handily tunable electronic energy levels, broad absorption spectra, narrow band gaps and high charge carrier mobilities.^[5–9] D-A type conjugated polymers are generally constructed by the alternating copolymerization between the electron-rich (D) building blocks and electron-deficient (A) building blocks. The electron-donating and electron-withdrawing capacities of the D and A building blocks, respectively, have a great impact on the energy levels and band gaps of the D-A polymers.^[10] To now, the common D units are often the electron-rich thienyl and phenyl moieties, such as fluorene,^[11] carbazole,^[12] cyclopentadithiophene,^[13] benzodithiophene^[14,15] and indacenodithiophene.^[16,17] The

popular A units are mainly based on the strong electron-withdrawing groups, such as imide,^[18,19] amide,^[20,21] thiadiazole,^[22,23] cyano groups,^[24] and boron-nitrogen coordination bonds (B←N).^[25–28] However, the type and number of A units those have been reported so far are still limited because the introduction of strong electron-withdrawing substituent limits the further modifiability of the backbone. Therefore, the development of synthetic strategies for novel A building blocks is important in the diversification of D-A type conjugated polymers.

Organoboron chemistry provides a powerful toolbox for the design of conjugated polymers. These conjugated polymers based on B←N units have already been applied to a variety of organic optoelectronic devices and achieved excellent device performance, such as OSCs, OFETs and organic thermoelectrics.^[26,27,29–33] The electron-deficient nature of B←N units can be attributed to not only the electronic structure of coordination bonds but also the electron-withdrawing substituents on the boron atoms.^[34–36] In the vast majority of cases, the boron atoms are substituted with fluorine atoms.^[26,27,29,37,38] Additionally, a few B←N units are functionalized with phenyl groups on the boron atoms.^[28,31] The electron-withdrawing cyano groups, one of the efficient design strategies for A units, can significantly decrease the LUMO and HOMO energy levels of the resulting building blocks when introduced into π -conjugated skeletons.^[39] Thus, by combining the B←N bonds with cyano groups in a π -conjugated skeleton is expected to obtain a stronger A building

* Corresponding author, E-mail: liujun@ciac.ac.cn

† These authors contributed equally to this work.

Special Issue: In Memory of Professor Fosong Wang

Received November 29, 2022; Accepted December 26, 2022; Published online March 2, 2023

block.

In this study, we focused on the newly developed N←B←N based building block (**SBN-1**) with a balanced resonance hybrid between B, N covalent and coordination bonds.^[40] The resonance of two B, N bonds endows **SBN-1** with excellent chemical stability and photostability. In order to enhance the electron affinity of **SBN-1**, the nucleophilic substitution reaction with trimethylsilyl cyanide (TMSCN) was conducted, leading to the cyano-substituted **SBN-3** (see Fig. 1a). Density functional theory (DFT) calculations and experimental results have confirmed that the replacement of the fluorine atoms with cyano groups can significantly decrease the LUMO and HOMO energy levels of **SBN-3**. In particular, the LUMO energy level of **SBN-3** is 0.36 eV lower than that of **SBN-1** as determined by cyclic voltammetry measurement. As a consequence, **SBN-3** exhibits a LUMO energy level as lower as −3.51 eV. In addition, due to the greater impact of cyano substitution on LUMO than on HOMO, **SBN-3** exhibits a significantly reduced band gap, near-infrared absorption and fluorescence properties. Considering the strong electron-deficient nature of **SBN-3**, we transformed it into the di-bromo monomer and further prepared two D-A polymers *via* Stille polymerization between the resultant monomer and thiophene-based D units. The two polymers both show small optical band gaps of *ca.* 1.3 eV. This work thus provides not only an effective approach to design strong A units but also a new electron-deficient building block for D-A type conjugated polymers.

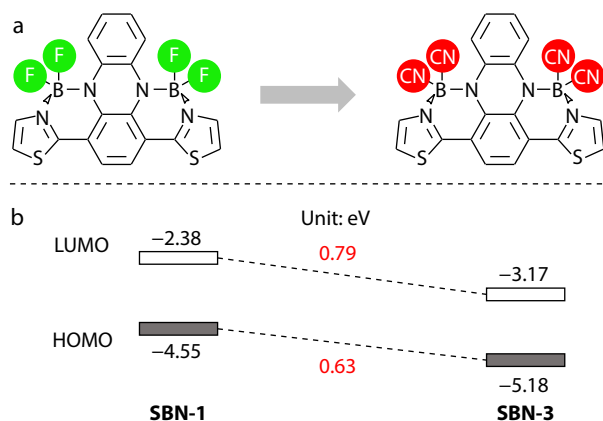


Fig. 1 (a) Schematic diagram of the chemical structures of **SBN-1** and **SBN-3**; (b) The calculated LUMO/HOMO energy levels of **SBN-1** and **SBN-3** at the B3LYP/6-31G(d, p) level.

EXPERIMENTAL

Materials

All solvents and reagents were purchased from commercial sources and used without further purification unless otherwise noted. Anhydrous CH_2Cl_2 was used as received. Anhydrous toluene was dried over sodium and distilled prior to use. Compounds **1** and **2** were prepared following the previously reported methods.^[40]

Synthesis

Synthesis of **SBN-1**

Compound **1** (75 mg, 0.15 mmol) was dissolved in anhydrous

CH_2Cl_2 (10 mL) under an argon atmosphere and heated to 50 °C, and then $\text{BF}_3 \cdot \text{Et}_2\text{O}$ (0.77 mL, 5.78 mmol) and Et_3N (0.41 mL, 2.93 mmol) were added dropwise *via* syringe. The resulting mixture was stirred for 4 h at 50 °C. After cooling to room temperature, the mixture was extracted with CH_2Cl_2 and water. The organic layer was washed with brine for three times and dried over Na_2SO_4 . After removing the solvent by evaporation, the residue was purified by silica gel column chromatography using CH_2Cl_2 /petroleum ether (1:1, V:V) as the eluent. **SBN-1** was obtained as a dark green solid in 86% yield (76 mg, 0.12 mmol). $^1\text{H-NMR}$ (500 MHz, C_6D_6 , δ , ppm): 8.34 (s, 2H), 7.25 (s, 2H), 6.84 (s, 2H), 5.95 (s, 2H), 1.99 (t, $J=7.5$ Hz, 4H), 1.21 (dt, $J=14.1$, 7.0 Hz, 4H), 1.15–0.95 (m, 12H), 0.90 (t, $J=7.3$ Hz, 6H). Anal. Calcd. for $\text{C}_{30}\text{H}_{34}\text{B}_2\text{F}_4\text{N}_4\text{S}_2$: C, 58.84; H, 5.60; B, 3.53; F, 12.41; N, 9.15; S, 10.47. Found: C, 58.72; H, 5.76; N, 9.04.

Synthesis of **SBN-3**

To a solution of **SBN-1** (50 mg, 0.08 mmol) in anhydrous CH_2Cl_2 (10 mL) under an argon atmosphere were added SnCl_4 (9.6 μL , 0.08 mmol) and trimethylsilyl cyanide (TMSCN) (0.22 mL, 1.63 mmol) dropwise *via* syringe. After stirring at 25 °C for 3 h, the reaction was quenched with water and extracted with CH_2Cl_2 (2 \times 25 mL). The combined organic layers were washed with a saturated solution of NaHCO_3 (2 \times 25 mL), distilled water (2 \times 25 mL) and dried over Na_2SO_4 . After removing the solvent by evaporation, the residue was purified by silica gel column chromatography using CH_2Cl_2 as the eluent. **SBN-3** was obtained as a green solid in 82% yield (43 mg, 0.07 mmol). $^1\text{H-NMR}$ (500 MHz, CDCl_3 , δ , ppm): 7.65 (s, 2H), 7.33 (dd, $J=6.1$, 3.4 Hz, 2H), 7.05 (s, 2H), 6.42 (s, 2H), 2.90 (t, $J=7.5$ Hz, 4H), 1.80–1.73 (m, 4H), 1.48–1.42 (m, 4H), 1.38–1.32 (m, 8H), 0.92 (t, 6H). $^{13}\text{C-NMR}$ (101 MHz, CDCl_3 , δ , ppm): 162.97, 140.56, 131.85, 131.41, 125.01, 117.68, 117.30, 107.89, 77.36, 77.04, 76.72, 31.28, 30.68, 28.65, 27.38, 22.43, 14.00. Anal. Calcd. for $\text{C}_{34}\text{H}_{34}\text{B}_2\text{N}_8\text{S}_2$: C, 63.76; H, 5.35; B, 3.38; N, 17.50; S, 10.01. Found: C, 63.70; H, 5.39; N, 17.45.

Synthesis of compound **3**

Compound **3** was prepared and purified in a procedure similar to that of **SBN-1** as a dark green solid in 81% yield. $^1\text{H-NMR}$ (500 MHz, C_6D_6 , δ , ppm): 8.32 (dd, $J=6.2$, 3.2 Hz, 2H), 7.43 (s, 2H), 6.85 (dd, $J=6.2$, 3.2 Hz, 2H), 3.81 (d, $J=7.4$ Hz, 4H), 2.24–2.08 (m, 2H), 1.58–1.29 (m, 64H), 0.95–0.91 (m, 12H). $^{13}\text{C-NMR}$ (126 MHz, C_6D_6 , δ , ppm): 158.93, 137.11, 136.35, 133.72, 132.15, 125.50, 120.28, 108.17, 103.13, 79.39, 38.62, 32.35, 31.73, 31.72, 30.66, 30.64, 30.25, 30.22, 30.17, 30.16, 29.89, 29.86, 27.27, 23.14, 23.13, 14.36. Anal. Calcd. for $\text{C}_{58}\text{H}_{88}\text{B}_2\text{Br}_2\text{F}_4\text{N}_4\text{O}_2\text{S}_2$: C, 58.30; H, 7.42; B, 1.81; Br, 13.37; F, 6.36; N, 4.69; O, 2.68; S, 5.37. Found: C, 58.25; H, 7.39; N, 4.78.

Synthesis of compound **4**

Compound **4** was prepared and purified in a procedure similar to that of **SBN-3** as a green solid in 80% yield. $^1\text{H-NMR}$ (500 MHz, C_6D_6 , δ , ppm): 7.89 (dd, $J=6.1$, 3.4 Hz, 2H), 7.43 (s, 2H), 6.74 (dd, $J=6.2$, 3.4 Hz, 2H), 3.79 (d, $J=7.4$ Hz, 4H), 2.07 (s, 2H), 1.44–1.29 (m, 64H), 0.94 (d, $J=7.0$ Hz, 12H). $^{13}\text{C-NMR}$ (126 MHz, C_6D_6 , δ , ppm): 159.60, 137.58, 135.41, 134.35, 131.60, 128.44, 128.25, 128.06, 126.03, 118.81, 112.39, 104.69, 79.88, 38.97, 32.55, 31.81, 31.79, 30.85, 30.82, 30.44, 30.42, 30.38, 30.35, 30.07. Anal. Calcd. for $\text{C}_{62}\text{H}_{88}\text{B}_2\text{Br}_2\text{N}_8\text{O}_2\text{S}_2$: C, 60.89; H, 7.25; B, 1.77; Br, 13.07; N, 9.16; O, 2.62; S, 5.24. Found: C, 60.75; H, 7.29; N, 9.12.

Synthesis of PBN-T

To a 5 mL microwave vial, compound **4** (57.8 mg, 0.047 mmol), 2,5-bis(trimethylstannyl)thiophene (19.23 mg, 0.047 mmol), Pd₂(dba)₃ (1.3 mg, 0.001 mmol) and P(*o*-Tol)₃ (3.5 mg, 0.011 mmol) were added. The vial was transferred into a nitrogen filled glovebox and anhydrous toluene (1 mL) was added. Then, the vial was sealed, subjected to a microwave reactor and heated at 120 °C for 2 h. After cooling to room temperature, the reaction mixture was poured into methanol. The resulting precipitate was collected and dried under vacuum to afford **PBN-T** as a brick-red solid in 64% yield (35.2 mg). *M_n*=3.5 kDa, *M_w*=6.5 kDa, PDI=1.8. Anal. Calcd for C₆₆H₉₂B₂N₈O₂S₃: C, 69.09; H, 8.08; B, 1.88; N, 9.77; O, 2.79; S, 8.38. Found: C, 69.25; H, 8.12; N, 9.65.

Synthesis of PBN-2T

PBN-2T was prepared from compound **4** (52.0 mg, 0.043 mmol) and 5,5'-bis(trimethylstannyl)-2,2'-bithiophene (20.9 mg, 0.043 mmol) in a procedure similar to that of **PBN-T**. The polymer was obtained as a dark red solid in 96% yield (50.6 mg). *M_n*=10.3 kDa, *M_w*=18.0 kDa, PDI=1.7. Anal. Calcd for C₇₀H₉₄B₂N₈O₂S₄: C, 68.39; H, 7.71; B, 1.76; N, 9.11; O, 2.60; S, 10.43. Found: C, 68.23; H, 7.79; N, 9.23.

RESULTS AND DISCUSSION

Synthesis and Characterization of SBN-3

The chemical structures and synthetic routes of **SBN-3** were depicted in Scheme 1. Starting material **1** was prepared according to literature methods.^[40] Direct borylation of **1** with BF₃·Et₂O and Et₃N afforded **SBN-1**, which might be regarded as a control compound. Subsequently, **SBN-3** was synthesized by a nucleophilic substitution reaction of **SBN-1** with TMSCN in the presence of SnCl₄.^[41,42]

The LUMO and HOMO energy levels of the model compounds of **SBN-1** and **SBN-3** were estimated by DFT calculations

at the B3LYP/6-31G(d, p) level. As shown in Fig. 1(b), the replacement of fluorine atoms with cyano groups can decrease the LUMO and HOMO energy levels by 0.79 eV and 0.63 eV, respectively. Thus, the corresponding bandgap is reduced by 0.16 eV. The lower energy levels can be ascribed to the stronger electron-withdrawing character of cyano groups than fluorine atoms. The optimized structures of **SBN-3** and **SBN-1** are shown in Fig. S1 (in the electronic supplementary information, ESI). The replacement of fluorine atoms with cyano groups endows **SBN-3** with a more planar geometry. A distinguishing characteristic of this unit is the balanced resonance hybrid of the B–N and B←N bond. The optimized geometry of **SBN-3** shows approximately equal bond lengths of B–N and B←N, which are close to ca. 1.56 Å. This suggests that the cyano groups substitution has a negligible effect on the resonance hybrid of the B–N and B←N. Interestingly, the cyano-substituted **SBN-3** has a large molecular dipole of 12.4 Debye, which is substantially higher compared to the 6.8 Debye of the fluorine-substituted **SBN-1**. This large dipole is also extremely rare in organic compounds. Furthermore, **SBN-3** possesses the similar LUMO/HOMO orbital distribution characteristics as **SBN-1**, its HOMO and LUMO are well delocalized in the whole conjugated skeleton (Fig. S2 in ESI).^[40] This indicates that the incorporation of cyano groups maintained the excellent electron delocalization characteristic of this B←N unit. The well electron delocalization in **SBN-3** is also verified by the nuclear independent chemical shift (NICS) values of the aromatic rings in **SBN-3** and **SBN-1** (Fig. S3 in ESI). The NICS(1)_{zz} values of all the aromatic rings in **SBN-3** are nearly equal to those of the aromatic rings in **SBN-1**, suggesting the two molecules have similar electron delocalization properties.

Fig. 2(a) shows the cyclic voltammetry (CV) curves of **SBN-1** and **SBN-3** in THF solutions. **SBN-1** displays a quasi-reversible reduction wave and two oxidation waves, while after the

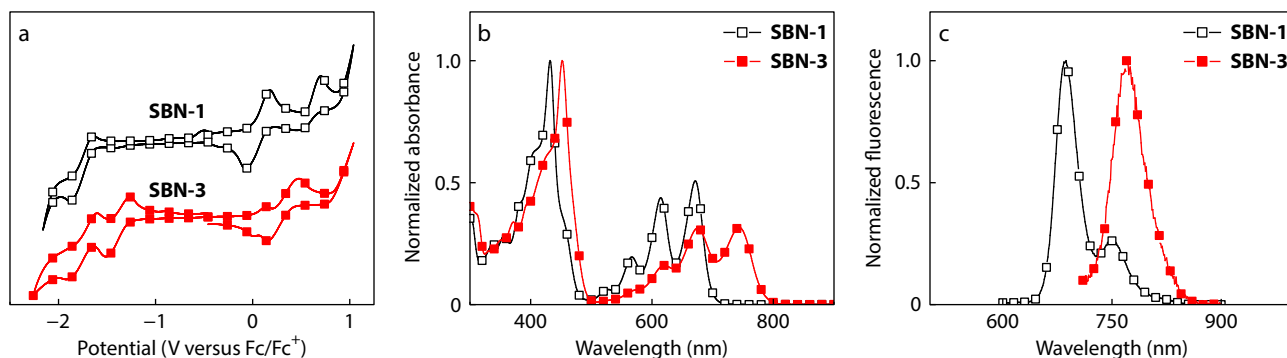
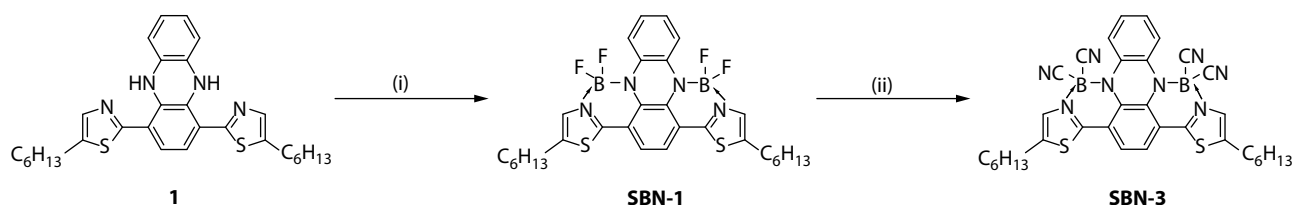


Table 1 Photophysical and electrochemical properties of **SBN-1** and **SBN-3**.

Compound	λ_{abs}^a (nm)	$E_g^{\text{opt}^a}$ (eV)	λ_{em}^a (nm)	E_{LUMO}^b (eV)	E_{HOMO}^b (eV)	$E_g^{\text{elec}^b}$ (eV)
SBN-1 [40]	432/614/671	1.78	687	-3.15	-4.80	1.65
SBN-3	452/676/744	1.58	770	-3.51	-5.01	1.50

^a Measured in dilute toluene solution; ^b $E_{\text{HOMO}}/E_{\text{LUMO}} = -(4.80 + E_{\text{onset}}^{\text{ox}}/E_{\text{onset}}^{\text{red}})$ eV.

cyano substitution, **SBN-3** displays two quasi-reversible reduction waves and two oxidation waves. The reported data of **SBN-1** are directly summarized in Table 1. The onset reduction potentials versus Fc/Fc⁺ of **SBN-3** are -1.65 and -1.29 V, respectively. The onset oxidation potentials versus Fc/Fc⁺ of **SBN-3** are 0.00 and 0.21 V, respectively. According to the onset potentials of the reduction and oxidation, the LUMO and HOMO energy levels of **SBN-3** are estimated to be -3.51 and -5.01 eV, respectively. In comparison to those of **SBN-1**, the LUMO and HOMO energy levels of **SBN-3** are lowered by 0.36 and 0.21 eV, respectively. The downshifted LUMO and HOMO energy levels are due to the stronger electron-withdrawing effect of the cyano groups. Moreover, the cyano groups exhibit a more significant influence on LUMO than HOMO, leading to a smaller electrochemical band gap of 1.50 eV. These results are in accordance with DFT calculation results.

Fig. 2(b) shows the absorption spectra of **SBN-1** and **SBN-3** in dilute toluene solution, and the corresponding data are collected in Table 1. Both of them display multiple absorption bands in the range of 300 nm to 800 nm. The absorption peaks at long-wavelength region of **SBN-1** and **SBN-3** are associated with the HOMO → LUMO transition according to the TD-DFT calculations (see Table S5 in ESI). Compared with those of **SBN-1**, the absorption peaks of **SBN-3** significantly red-shifted, which are located at 452 nm/620 nm/676 nm/744 nm. According to the onset values of their absorption in solutions, the optical bandgaps are calculated to be 1.78 eV for **SBN-1** and 1.58 eV for **SBN-3**. The optical bandgap of **SBN-3** is narrower than that of **SBN-1** by 0.2 eV, which is consistent with the electrochemical band gaps obtained by CV. Fig. 2(c) shows the fluorescence spectra of the two compounds. **SBN-3** exhibits an emission peak at 770 nm, which is remarkably redshifted than the emission peak of **SBN-1** at 687 nm. These

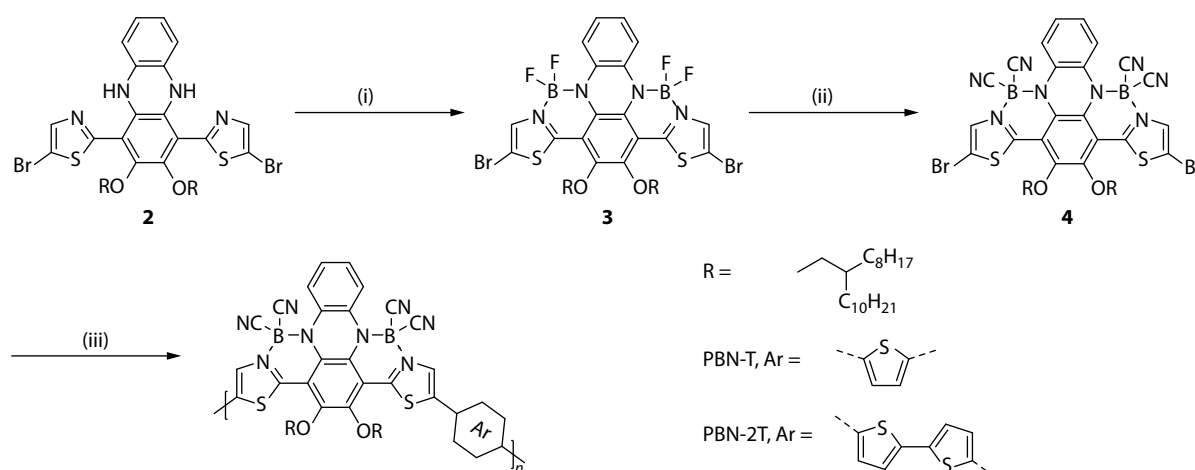
results indicate that the replacement of the fluorine atoms with cyano groups decreased the band gap of **SBN-3** and realized the absorption and emission in the NIR region.

Synthesis and Characterization of Polymers

Based on the strong electron-deficient property of cyano-substituted **SBN-3** building block, we selected thiophene and dithiophene as the D units to prepare D-A type conjugated polymers. To construct D-A polymers based on **SBN-3**, it is essential to incorporate reactive groups into its skeleton to obtain the monomer. Scheme 2 represents the chemical structure and synthetic route of the key di-bromo monomer **4**. We succeeded to attach bromines to the 5-position of the thiazole. To ensure the solubility of **4** and the resulting polymers, two long branched alkoxy chains were introduced to the central phenyl unit in **4**. Subsequently, we prepared two polymers, **PBN-T** and **PBN-2T**, via Stille polymerization of **4** and ditrimethylstannyl thiophene or ditrimethylstannyl 2,2'-bithiophene. According to the gel permeation chromatography (GPC), the number average molecular weight (M_n) and polydispersity index (PDI) are 3.5 kDa and 1.84 for **PBN-T** and 10.4 kDa and 1.74 for **PBN-2T**.

It was found that the two polymers can be easily dissolved in common organic solvents, such as toluene, chloroform and chlorobenzene. The decomposition temperature (T_d) of **PBN-T** and **PBN-2T** are both above 220 °C, as revealed by thermal gravimetric analysis (TGA).

DFT calculations at the B3LYP/6-31G(d, p) level were conducted to gain insights into the electronic structures of the polymers based on the cyano-substituted B←N unit. To simplify the computation, we chose the dimers of **PBN-T** and **PBN-2T** (**BN-T** and **BN-2T**) as model compounds, in which the long branched alkoxy chains are replaced with methoxyl



Scheme 2 The chemical structures and synthetic routes of the di-bromo monomer **4** and the two polymers, **PBN-T** and **PBN-2T**. Reagents and conditions: (i) $\text{BF}_3 \cdot \text{Et}_2\text{O}$, Et_3N , CH_2Cl_2 , 50 °C; (ii) SnCl_4 , TMSCN , CH_2Cl_2 , 25 °C; (iii) tris(dibenzylideneacetone)dipalladium(0), $\text{P}(o\text{-tol})_3$, toluene, 120 °C, microwave-assisted, 300 W.

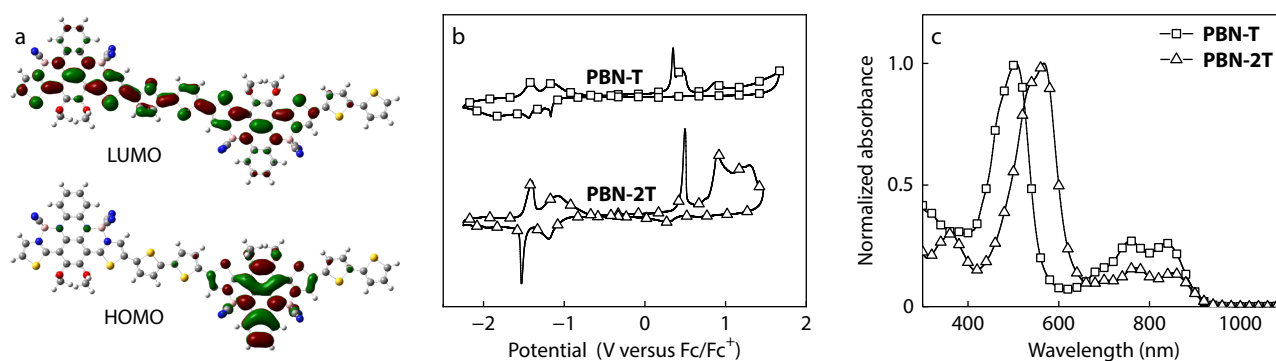


Fig. 3 (a) Kohn-Sham LUMO/HOMO of the model compound of **PBN-2T**; (b) Cyclic voltammograms of **PBN-T** and **PBN-2T** as thin film; (c) Normalized UV/Vis absorption of **PBN-T** and **PBN-2T** in dilute toluene solution (1×10^{-5} mol/L).

Table 2 Photophysical and electrochemical properties of **PBN-T** and **PBN-2T**.

Polymer	$\lambda_{\text{abs}}^{\text{sol a}}$ (nm)	$\epsilon^{\text{a,b}}$ ($\text{M}^{-1} \cdot \text{cm}^{-1}$)	$\lambda_{\text{abs}}^{\text{film}}$ (nm)	$E_{\text{g}}^{\text{opt c}}$ (eV)	$E_{\text{LUMO}}^{\text{d}}$ (eV)	$E_{\text{HOMO}}^{\text{d}}$ (eV)
PBN-T	505/757/838	22, 587	505/754/829	1.35	-3.69	-5.11
PBN-2T	567/768/851	41, 255	562/775/861	1.31	-3.77	-5.23

^a Measured in dilute toluene solution; ^b Determined at the highest peak wavelength; ^c Measured in thin film; ^d $E_{\text{HOMO}}/E_{\text{LUMO}} = -(4.80 + E_{\text{onset}}^{\text{ox}}/E_{\text{onset}}^{\text{red}})$ eV.

groups. **BN-T** and **BN-2T** exhibit similar electronic structures in their LUMO and HOMO distributions, as shown in Fig. 3(a) and Fig. S5 (in ESI). Their LUMOs are delocalized evenly along the backbone, while the HOMOs are mainly localized on the cyano-substituted B←N unit. These characteristics are rare in D-A polymers, which usually show delocalized HOMOs and localized LUMOs.^[15,43,44] The electronic structure of **BN-T** and **BN-2T** is anticipated to significantly impact their opto-electronic properties.

Fig. 3(b) shows the CV curves of **PBN-T** and **PBN-2T**. The two polymers both possess multiple irreversible oxidation waves and reversible reduction waves. The LUMO and HOMO energy levels estimated from the onset reduction and oxidation waves are -3.69 and -5.11 eV for **PBN-T** and -3.77 and -5.23 eV for **PBN-2T**. Thus, the electrochemical band gaps of **PBN-T** and **PBN-2T** are calculated as 1.42 and 1.46 eV. The LUMO energy levels of both polymers are much lower than the HOMO energy levels, compared to the compound **SBN-3**. This difference is due to the delocalized LUMOs and localized HOMOs of both polymers, which has been demonstrated by B←N based polymers with similar electronic structures.^[40,45]

Fig. 3(c) shows the absorption spectra of **PBN-T** and **PBN-2T** in dilute toluene solution, the corresponding data are summarized in Table 2. The two polymers display similar spectra shapes as the small molecule **SBN-3**. The maximum absorption peak of **PBN-T** is located at 507 nm and the longest-wavelength absorption peak is at 836 nm. While, **PBN-2T** shows an absorption maximum at 567 nm with the longest-wavelength absorption peak at 851 nm. The absorption at 700–900 nm for **PBN-T** is stronger than that of **PBN-2T** owing to the higher overlap extent between the LUMO and HOMO distributions for **PBN-T** (Fig. 3a and Fig. S5 in ESI).^[46] The optical band gaps are 1.35 eV for **PBN-T** and 1.31 eV for **PBN-2T** as calculated from the absorption onsets of the thin films (see Fig. S6 in ESI). Compared with the small molecule **SBN-3**, the two polymers exhibit smaller optical band gaps owing to the extended π -conjugation in the polymers. These results imply that the use of the newly developed cyano-sub-

stituted B←N unit as the A building block is an effective way to construct D-A type conjugated polymers with narrow band gaps.

CONCLUSIONS

In summary, we developed a cyano-substituted organoboron electron-deficient building block for D-A type conjugated polymers. The replacement of fluorine atoms with cyano groups at the boron centers endows **SBN-3** with a lower LUMO energy level of -3.51 eV owing to the strong electron-withdrawing ability of cyano groups. Furthermore, **SBN-3** exhibits a considerably decreased band gap, due to the more substantial influence of cyano substitution on LUMO than on HOMO, leading to NIR absorption and fluorescence characteristics. By using the cyano-substituted B←N unit as the A building block, two D-A conjugated polymers have been further prepared. The resulting polymers exhibit narrow optical band gaps of ca. 1.3 eV as well as distinctive electronic structures, *i.e.*, delocalized LUMOs and localized HOMOs. This work thus provides not only an effective approach to design strong acceptor units but also a new electron-deficient building block for D-A type conjugated polymers.

NOTES

The authors declare no competing financial interest.

Electronic Supplementary Information

Electronic supplementary information (ESI) is available free of charge in the online version of this article at <http://doi.org/10.1007/s10118-023-2940-4>.

ACKNOWLEDGMENTS

This work was financially supported by the National Natural

Science Foundation of China (Nos. 22135007, 21875244 and 52073281) and Jilin Scientific and Technological Development Program (No. YDZJ202101ZYTS138).

REFERENCES

- Grimsdale, A. C.; Chan, K. L.; Martin, R. E.; Jokisz, P. G.; Holmes, A. B. Synthesis of light-emitting conjugated polymers for applications in electroluminescent devices. *Chem. Rev.* **2009**, *109*, 897–1091.
- Wang, Z. L.; Shi, Y. B.; Deng, Y. F.; Han, Y.; Geng, Y. H. Toward high mobility green solvent-processable conjugated polymers: a systematic study on chalcogen effect in poly(diketopyrrolopyrrole-*alt*-terchalcogenophene)s. *Adv. Funct. Mater.* **2021**, *31*, 2104881.
- Genene, Z.; Mammo, W.; Wang, E. G.; Andersson, M. R. Recent advances in n-type polymers for all-polymer solar cells. *Adv. Mater.* **2019**, *31*, 180727.
- Shi, K.; Zhang, F. J.; Di, C. A.; Yan, T. W.; Zou, Y.; Zhou, X.; Zhu, D. B.; Wang, J. Y.; Pei, J. Toward high performance n-type thermoelectric materials by rational modification of BDPPV backbones. *J. Am. Chem. Soc.* **2015**, *137*, 6979–6982.
- Kim, M.; Ryu, S. U.; Park, S. A.; Choi, K.; Kim, T.; Chung, D.; Park, T. Donor-acceptor-conjugated polymer for high-performance organic field-effect transistors: a progress report. *Adv. Funct. Mater.* **2020**, *30*, 190454.
- Cao, X.; Min, Y.; Tian, H. K.; Liu, J. Incorporating cyano groups to a conjugated polymer based on double B←N-bridged bipyridine units for unipolar n-type organic field-effect transistors. *Org. Mater.* **2021**, *3*, 469–476.
- Wang, M.; Hu, X. W.; Liu, P.; Li, W.; Gong, X.; Huang, F.; Cao, Y. Donor-acceptor conjugated polymer based on naphtho[1,2-*c*:5,6-*c'*]bis[1,2,5]thiadiazole for high-performance polymer solar cells. *J. Am. Chem. Soc.* **2011**, *133*, 9638–9641.
- Cheng, P.; Yang, Y. Narrowing the band gap: the key to high-performance organic photovoltaics. *Acc. Chem. Res.* **2020**, *53*, 1218–1228.
- Vella, J. H.; Huang, L. F.; Eedugurala, N.; Mayer, K. S.; Ng, T. N.; Azoulay, J. D. Broadband infrared photodetection using a narrow bandgap conjugated polymer. *Sci. Adv.* **2021**, *7*, eabg2418.
- Dou, L. T.; Liu, Y. S.; Hong, Z. R.; Li, G.; Yang, Y. Low-bandgap near-IR conjugated polymers/molecules for organic electronics. *Chem. Rev.* **2015**, *115*, 12633–12665.
- Wang, X. J.; Perzon, E.; Delgado, J. L.; de la Cruz, P.; Zhang, F. L.; Langa, F.; Andersson, M.; Inganäs, O. Infrared photocurrent spectral response from plastic solar cell with low-band-gap polyfluorene and fullerene derivative. *Appl. Phys. Lett.* **2004**, *85*, 5081–5083.
- Blouin, N.; Michaud, A.; Leclerc, M. A low-bandgap poly(2,7-carbazole) derivative for use in high-performance solar cells. *Adv. Mater.* **2007**, *19*, 2295–2300.
- Hu, X. M.; Zhong, C. X.; Li, X. Y.; Jia, X.; Wei, Y.; Xie, L. H. Synthesis and application of cyclopentadithiophene derivatives. *Acta Chim. Sinica* **2021**, *79*, 953–966.
- Yao, H. F.; Ye, L.; Zhang, H.; Li, S. S.; Zhang, S. Q.; Hou, J. H. Molecular design of benzodithiophene-based organic photovoltaic materials. *Chem. Rev.* **2016**, *116*, 7397–7457.
- Bin, H. J.; Zhong, L.; Zhang, Z. G.; Gao, L.; Yang, Y. K.; Xue, L. W.; Zhang, J.; Zhang, Z. J.; Li, Y. F. Alkoxy substituted benzodithiophene-*alt*-fluorobenzotriazole copolymer as donor in non-fullerene polymer solar cells. *Sci. China Chem.* **2016**, *59*, 1317–1322.
- Li, Y. X.; Gu, M. C.; Pan, Z.; Zhang, B.; Yang, X. T.; Gu, J. W.; Chen, Y. Indacenodithiophene: a promising building block for high performance polymer solar cells. *J. Mater. Chem. A* **2017**, *5*, 10798–10814.
- Wadsworth, A.; Chen, H.; Thorley, K. J.; Cendra, C.; Nikolka, M.; Bristow, H.; Moser, M.; Salbeck, A.; Anthopoulos, T. D.; Sirringhaus, H.; McCulloch, I. Modification of indacenodithiophene-based polymers and its impact on charge carrier mobility in organic thin-film transistors. *J. Am. Chem. Soc.* **2020**, *142*, 652–664.
- Sun, H. L.; Wang, L.; Wang, Y. F.; Guo, X. G. Imide-functionalized polymer semiconductors. *Chem. Eur. J.* **2019**, *25*, 87–105.
- Chen, Z. C.; Zhang, Y.; Wang, P.; Yang, J. X.; Yang, K.; Li, J. F.; Yang, J.; Li, Y. C.; Dong, H. L.; Guo, X. G. A class of electron-deficient units: fluorenone imide and its electron-withdrawing group-functionalized derivatives. *Chem. Commun.* **2022**, *58*, 12467–12470.
- Lei, T.; Dou, J. H.; Cao, X. Y.; Wang, J. Y.; Pei, J. Electron-deficient poly(*p*-phenylene vinylene) provides electron mobility over 1 cm² V⁻¹ s⁻¹ under ambient conditions. *J. Am. Chem. Soc.* **2013**, *135*, 12168–12171.
- Wang, Y. Z.; Yu, Y. P.; Liao, H. L.; Zhou, Y. C.; McCulloch, I.; Yue, W. The chemistry and applications of heteroisoindigo units as enabling links for semiconducting materials. *Acc. Chem. Res.* **2020**, *53*, 2855–2868.
- Wang, C.; Liu, F.; Chen, Q. M.; Xiao, C. Y.; Wu, Y. G.; Li, W. W. Benzothiadiazole-based conjugated polymers for organic solar cells. *Chinese J. Polym. Sci.* **2021**, *39*, 525–536.
- Wang, Y.; Michinobu, T. Benzothiadiazole and its π -extended, heteroannulated derivatives: useful acceptor building blocks for high-performance donor-acceptor polymers in organic electronics. *J. Mater. Chem. C* **2016**, *4*, 6200–6214.
- Feng, K.; Guo, H.; Wang, J. W.; Shi, Y. Q.; Wu, Z.; Su, M. Y.; Zhang, X. H.; Son, J. H.; Woo, H. Y.; Guo, X. G. Cyano-functionalized bithiophene imide-based n-type polymer semiconductors: synthesis, structure-property correlations, and thermoelectric performance. *J. Am. Chem. Soc.* **2021**, *143*, 1539–1552.
- Wakamiya, A.; Taniguchi, T.; Yamaguchi, S. Intramolecular B-N coordination as a scaffold for electron-transporting materials: synthesis and properties of boryl-substituted thienylthiazoles. *Angew. Chem. Int. Ed.* **2006**, *45*, 3170–3173.
- Dou, C. D.; Long, X. J.; Ding, Z. C.; Xie, Z. Y.; Liu, J.; Wang, L. X. An electron-deficient building block based on the B←N unit: an electron acceptor for all-polymer solar cells. *Angew. Chem. Int. Ed.* **2016**, *55*, 1436–1440.
- Zhao, R. Y.; Dou, C. D.; Liu, J.; Wang, L. X. An alternating polymer of two building blocks based on B←N unit: non-fullerene acceptor for organic photovoltaics. *Chinese J. Polym. Sci.* **2017**, *35*, 198–206.
- Dou, C. D.; Ding, Z. C.; Zhang, Z. J.; Xie, Z. Y.; Liu, J.; Wang, L. X. Developing conjugated polymers with high electron affinity by replacing a C-C unit with a B←N unit. *Angew. Chem. Int. Ed.* **2015**, *54*, 3648–3652.
- Miao, J. H.; Wang, Y. H.; Liu, J.; Wang, L. X. Organoboron molecules and polymers for organic solar cell applications. *Chem. Soc. Rev.* **2022**, *51*, 153–187.
- Dong, C. S.; Deng, S. H.; Meng, B.; Liu, J.; Wang, L. X. A distannylated monomer of a strong electron-accepting organoboron building block: enabling acceptor-acceptor-type conjugated polymers for n-type thermoelectric applications. *Angew. Chem. Int. Ed.* **2021**, *60*, 16184–16190.
- Li, Y. C.; Meng, H. F.; Liu, T.; Xiao, Y. Q.; Tang, Z. H.; Pang, B.; Li, Y. Q.; Xiang, Y.; Zhang, G. Y.; Lu, X. H.; Yu, G.; Yan, H.; Zhan, C. L.; Huang, J. H.; Yao, J. N. 8.78% Efficient all-polymer solar cells enabled by polymer acceptors based on a B←N embedded electron-deficient unit. *Adv. Mater.* **2019**, *31*, 1904585.
- Xiang, Y.; Meng, H. F.; Yao, Q.; Chang, Y.; Yu, H.; Guo, L.; Xue, Q. F.; Zhan, C. L.; Huang, J. H.; Chen, G. H. B←N bridged polymer

- acceptors with 900 nm absorption edges enabling high-performance all-polymer solar cells. *Macromolecules* **2020**, *53*, 9529–9538.
- 33 Huang, J. H.; Wang, X. L.; Xiang, Y.; Guo, L.; Chen, G. H. B←N coordination: from chemistry to organic photovoltaic materials. *Adv. Energy Sustain. Res.* **2021**, *2*, 2100016.
- 34 Cao, Y. R.; Zhu, C. Z.; Barlog, M.; Barker, K. P.; Ji, X. Z.; Kalin, A. J.; Al-Hashimi, M.; Fang, L. Electron-deficient polycyclic π -system fused with multiple B←N coordinate bonds. *J. Org. Chem.* **2021**, *86*, 2100–2106.
- 35 Shao, X. X.; Wang, J. H.; Marder, T. B.; Xie, Z. Y.; Liu, J.; Wang, L. X. N–B←N bridged bithiophene: a building block with reduced band gap to design n-type conjugated polymers. *Macromolecules* **2021**, *54*, 6718–6725.
- 36 Gapare, R. L.; Thompson, A. Substitution at boron in BODIPYs. *Chem. Commun.* **2022**, *58*, 7351–7359.
- 37 Yoshii, R.; Yamane, H.; Tanaka, K.; Chujo, Y. Synthetic strategy for low-band gap oligomers and homopolymers using characteristics of thiophene-fused boron dipyrromethene. *Macromolecules* **2014**, *47*, 3755–3760.
- 38 Zhang, Z.; Yuan, D. F.; Liu, X. S.; Kim, M. J.; Nashchadin, A.; Sharapov, V.; Yu, L. P. BODIPY-containing polymers with ultralow band gaps and ambipolar charge mobilities. *Macromolecules* **2020**, *53*, 2014–2020.
- 39 Kim, H. S.; Huseynova, G.; Noh, Y. Y.; Hwang, D. H. Modulation of majority charge carrier from hole to electron by incorporation of cyano groups in diketopyrrolopyrrole-based polymers. *Macromolecules* **2017**, *50*, 7550–7558.
- 40 Shao, X. X.; Liu, M. Y.; Liu, J.; Wang, L. X. A resonating B, N covalent bond and coordination bond in aromatic compounds and conjugated polymers. *Angew. Chem. Int. Ed.* **2022**, *61*, e202205893.
- 41 Nguyen, A. L.; Wang, M. D.; Bobadova-Parvanova, P.; Do, Q.; Zhou, Z. H.; Fronczek, F. R.; Smith, K. M.; Vicente, M. G. H. Synthesis and properties of B-cyano-BODIPYs. *J. Porphyrins Phthalocyanines* **2016**, *20*, 1409–1419.
- 42 Li, L. L.; Nguyen, B.; Burgess, K. Functionalization of the 4,4-difluoro-4-bora-3a,4a-diaza-s-indacene (BODIPY) core. *Bioorg. Med. Chem. Lett.* **2008**, *18*, 3112–3116.
- 43 Ma, S. S.; Song, Y.; Wang, Z. F.; He, B. T.; Yang, X. Y.; Li, L.; Xu, B. M.; Zhang, J.; Huang, F.; Cao, Y. Synthesis of medium bandgap copolymers based on benzotriazole for non-fullerene organic solar cells. *Polymer* **2019**, *179*, 121580.
- 44 Yan, H.; Chen, Z. H.; Zheng, Y.; Newman, C.; Quinn, J. R.; Dotz, F.; Kastler, M.; Facchetti, A. A high-mobility electron-transporting polymer for printed transistors. *Nature* **2009**, *457*, 679–686.
- 45 Shao, X. X.; Dou, C. D.; Liu, J.; Wang, L. X. A new building block with intramolecular D-A character for conjugated polymers: ladder structure based on B←N unit. *Sci. China Chem.* **2019**, *62*, 1387–1392.
- 46 Wang, Y. H.; Wang, N.; Yang, Q. Q.; Zhang, J. D.; Liu, J.; Wang, L. X. A polymer acceptor containing the B←N unit for all-polymer solar cells with 14% efficiency. *J. Mater. Chem. A* **2021**, *9*, 21071–21077.